Available online at www.sciencedirect.com

ScienceDirect

Polymer 48 (2007) 5681−5687

polymer

www.elsevier.com/locate/polymer

Effects of solvent on microstructure and proton conductivity of organic−inorganic hybrid membranes

Haruyoshi Sato [a], Tomohisa Norisuye [a,*], Tsuyoshi Takemori [a], Qui Tran-Cong-Miyata [a], Shigeki Nomura [b]

[a] *Department of Macromolecular Science and Engineering, Graduate School of Science and Technology, Kyoto Institute of Technology Matsugasaki, Sakyo-ku, Kyoto 606-8585, Japan*

[b] *R&D Center, Sekisui Chemical Co., Ltd., 32 Wadai, Tsukuba-shi, Ibaraki 300-4292, Japan*

Received 6 March 2007; received in revised form 4 July 2007; accepted 25 July 2007

Abstract

Effects of solvent on the microscopic structure and proton conductivity of organic−inorganic hybrids containing heteropolyacid are reported. The organic−inorganic hybrids were prepared by sol−gel synthesis of 1,8-bis(triethoxysilyl)octane (TES-Oct) in the presence of phosphotungstic acid (PWA). The proton conductivity of the membranes prepared under different solvents exhibited greater values in the order methanol < 1-butanol < 2-propanol < ethanol < 1-propanol < 2-butanol. The conductivity strongly correlated to the amount of incorporated PWA in the membranes, which was determined by titration of the solutions containing PWA leaked from the membrane. Small-angle X-ray scattering (SAXS), atomic force microscopy (AFM) and thermogravimetric analysis (TGA) were employed to reveal the relationship between the proton conductivity and microscopic structure of the TES-Oct/PWA membranes. It was found that there is an optimal condition for the formation of the condensed domain structure, indicating the important role of the structures in the membrane conductivity.

Keywords: Sol−gel; Proton conductivity; Scattering

1. Introduction

The sol−gel method has become a standard procedure to fabricate a wide variety of materials, such as porous glasses and homogeneous particles with controllable sizes [1,2]. The principal reactions of this method, i.e., hydrolysis and condensation of alkoxysilanes, are generally controlled by an acid or a base catalyst to obtain a branched network structure or particles. Although the reaction can be fairly accelerated by addition of such catalysts, the sol−gel reaction can be crucially terminated by the cyclization of the adjacent alkoxyl groups due to the nature of multifunctional monomers [3−5]. The problem can be circumvented by a chemical modification of alkoxysilanes, e.g., introducing a molecular bridge into alkoxysilanes to maintain a moderate separation between the functional groups of the precursor [4,6]. This also opens a route to fabricate advanced materials with a well-defined architecture at the molecular level. For example, when the reaction is initiated by an alkoxysilane containing an organic segment as a starting compound, one can obtain an organic−inorganic hybrid with a certain organic/inorganic sequence in one step.

In our previous works [7], sol−gel reaction of 1,8-bis(triethoxysilyl)octane (TES-Oct) in the presence of phosphotungstic acid (PWA) was carried out in order to obtain organic−inorganic hybrids containing a polyacid as proton conductive membranes. Here, PWA had an important role not only as a proton conductor but also as a unique catalyst with the super strong acidity [8,9]. The reaction process was characterized by *in situ* dynamic light scattering, where

---

* Corresponding author. Tel./fax: +81 75 724 7853.
E-mail address: nori@kit.jp (T. Norisuye).

0032-3861/$ - see front matter © 2007 Elsevier Ltd. All rights reserved.
doi:10.1016/j.polymer.2007.07.060

anomalous time evolution of the correlation functions was observed. While sol–gel process of a basic system is characterized by particle growth, the primary particles of acidic systems are fairly small, leading to a chain extension growth to form a weakly branched network structure [10]. However, the PWA system exhibited significantly larger cluster size throughout the gelation process, which was characteristic of the basic rather than the acidic systems. Once the reaction process of the TES-Oct/PWA systems was found to resemble to that of the basic system, one has to consider how to produce the clusters containing a larger amount of PWA, which is an important element for the better proton conduction.

Alcohols are the commonly used solvents for the sol–gel reaction to perform a homogenous reaction. The reactivity of monomers depends on the type of alcohols and in principle decreases with increasing molecular weight because the acidity of catalyst depends on the solvent polarity. Therefore, methanol or ethanol may be one of the most popular solvents to carry out the sol–gel synthesis in practice. So far, there are only a few papers dealing the solvent effects in sol–gel process [11,12]. Since the acidity of the catalyst and nucleophilicity of the precursor are expected to be dependent on (1) the type of solvent and (2) the incorporated amount of PWA, the proton conductivity of the membranes will be affected by those factors as well. In this paper, we investigated the effects of alcohol on the microscopic structure and the proton conductivity of the organic–inorganic hybrid membranes.

2. Experimental section

2.1. Samples

1,8-Bis(triethoxysilyl)octane (TES-Oct; Gelest), $(OC_2H_5)_3$–Si–$(CH_2)_8$–Si–$(OC_2H_5)_3$ and phosphotungstic acid (PWA; Aldrich), $H_3PW_{12}O_{40}\cdot nH_2O$, were used in this study, where n is the number of hydrated water. Monohydric alcohols such as methanol, ethanol, 1-propanol, 2-propanol, 1-butanol and 2-butanol (Wako, Japan) were used as a diluent. The boiling point and viscosity at 30 °C taken from Ref. [13] are summarized in Table 1. TES-Oct was used after purification by distillation under reduced pressure at least three times. The reaction batch was prepared by adding the mixture PWA + water + IPA into the mixture TES-Oct + IPA to initiate the reaction. After vigorous stirring, the solution was filtered through a Teflon membrane with the pore size of 0.20 μm and was poured into a plastic Petri dish, followed by an aging period for 24 h at 30 °C. After solidification, the resulting membranes were further aged under saturated vapor pressure at 60 °C for another 24 h. The dried membranes were then carefully washed with and stored in distilled water prior to measurements. TES-Oct and PWA concentrations were kept at 18.67 wt% and [PWA]/[TES-Oct] = 0.10, respectively.

Table 1
The boiling point and viscosity data for various alcohols

	Boiling point (°C)	Viscosity (cp at 30 °C)
Methanol	64.5	0.51
Ethanol	78.3	0.99
1-Propanol	97.2	1.73
2-Propanol	82.2	1.77
1-Butanol	117.7	2.27
2-Butanol	99.5	2.50

The data were taken from Ref. [13].

2.2. Characterization

2.2.1. Small-angle X-ray scattering (SAXS)

SAXS measurements were performed on a X-ray diffraction instrument (Mac Science Co. Ltd., M18XHF22) equipped with two-dimensional imaging plate detector, a high flux Huxley-Holmes camera, and nickel filtered Cu Kα X-ray (24 mA, 50 kV, $\lambda = 0.154$ nm) at room temperature. The scattering intensities were accumulated for 3 h. The one-dimensional scattering functions were obtained by radially averaging the two-dimensional data after correction for the sample thickness, scattering volume and transmission.

2.2.2. Atomic force microscopy (AFM)

AFM was operated in tapping mode using a Digital Instruments Multimode AFM, controlled by a Nanoscope IIIa scanning probe microscope controller with an extender module. Commercially available silicon tip with a spring constant of 30–40 N/m, single beam cantilevers of 125 μm long and a typical radius of curvature in the range 5–10 nm was used at the resonance frequencies ranging from 310 to 340 kHz depending on cantilever. Both topography and phase images with various scan sizes 500, 1000, 2000, 4000 nm were collected using tapping mode with a scan rate of 1 Hz in ambient atmosphere at room temperature. These images were transformed into a single master curve of the power-spectrum after a second

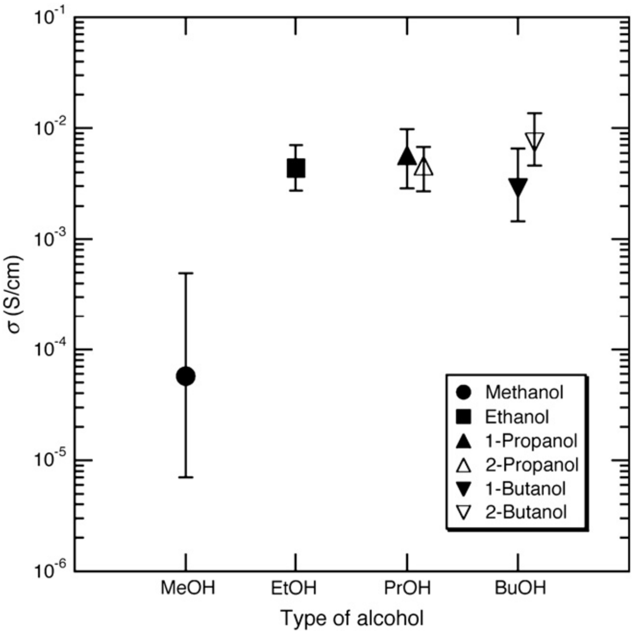

Fig. 1. The proton conductivity, σ, for the TES-Oct/PWA membranes prepared under different types of alcohol.

order background subtraction, fast Fourier transform (FFT) and radial averaging by homemade software [7].

2.2.3. Thermogravimetric analysis (TGA)

Thermogravimetric analysis (TGA) was conducted using a TGA2950 (TA Instruments thermogravimetric analyzer) with high-resolution mode. Sample weight was in the range 5−9 mg. Nitrogen was used as a purge gas. The heating rate was dynamically varied in response to the changes in the decomposition rate of the sample so as to improve the resolutions of the weight change. Maximum ramp heating rate was set at 20 °C/min.

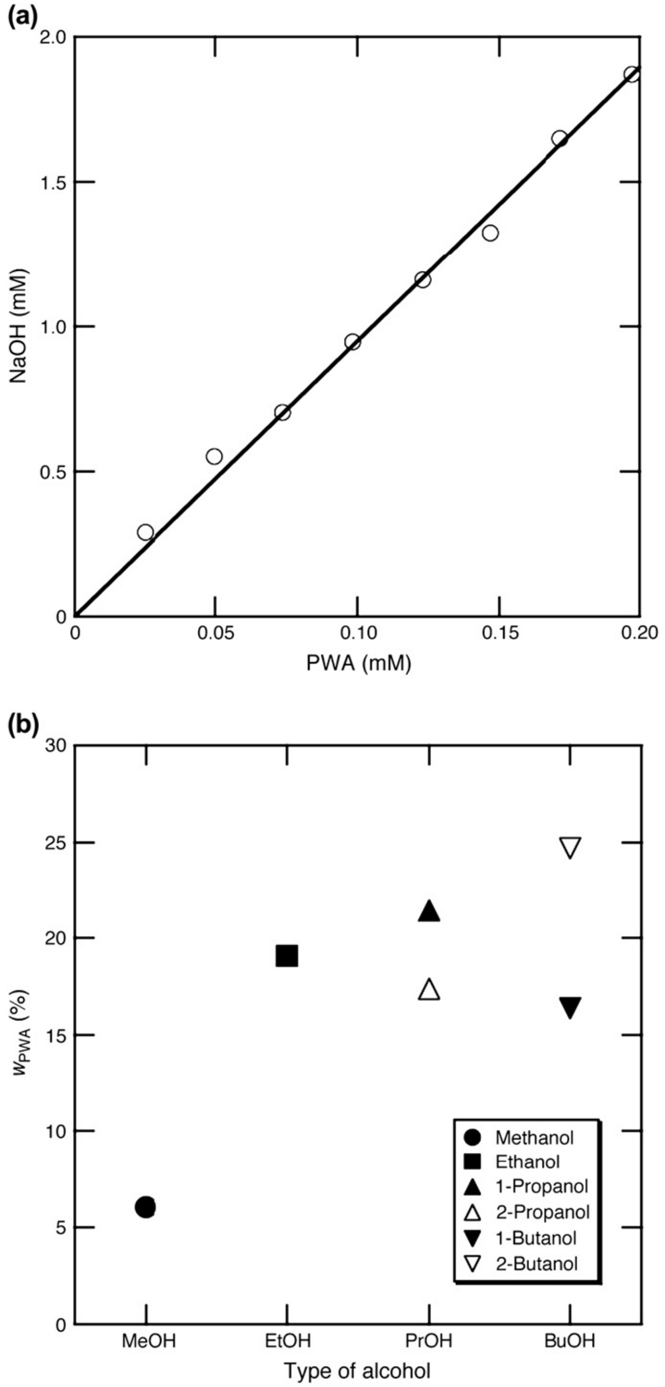

Fig. 2. (a) NaOH concentration required to neutralize PWA; (b) incorporated amount of PWA in the membranes for various types of solvent.

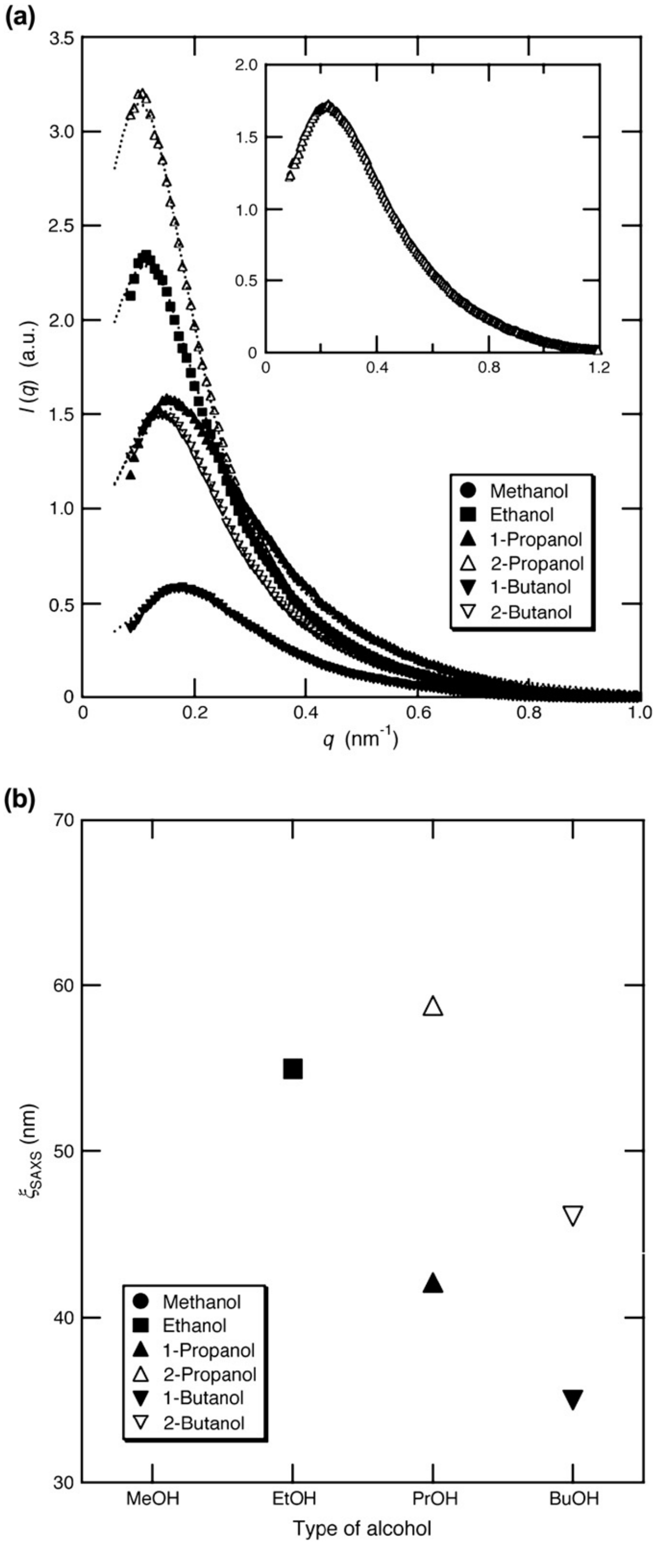

Fig. 3. (a) SAXS profile for the TES-Oct/PWA membranes synthesized in different solvents. The inset shows the SAXS profile for the HCl-catalyzed membrane. (b) ξ_{SAXS} for various types of solvent.

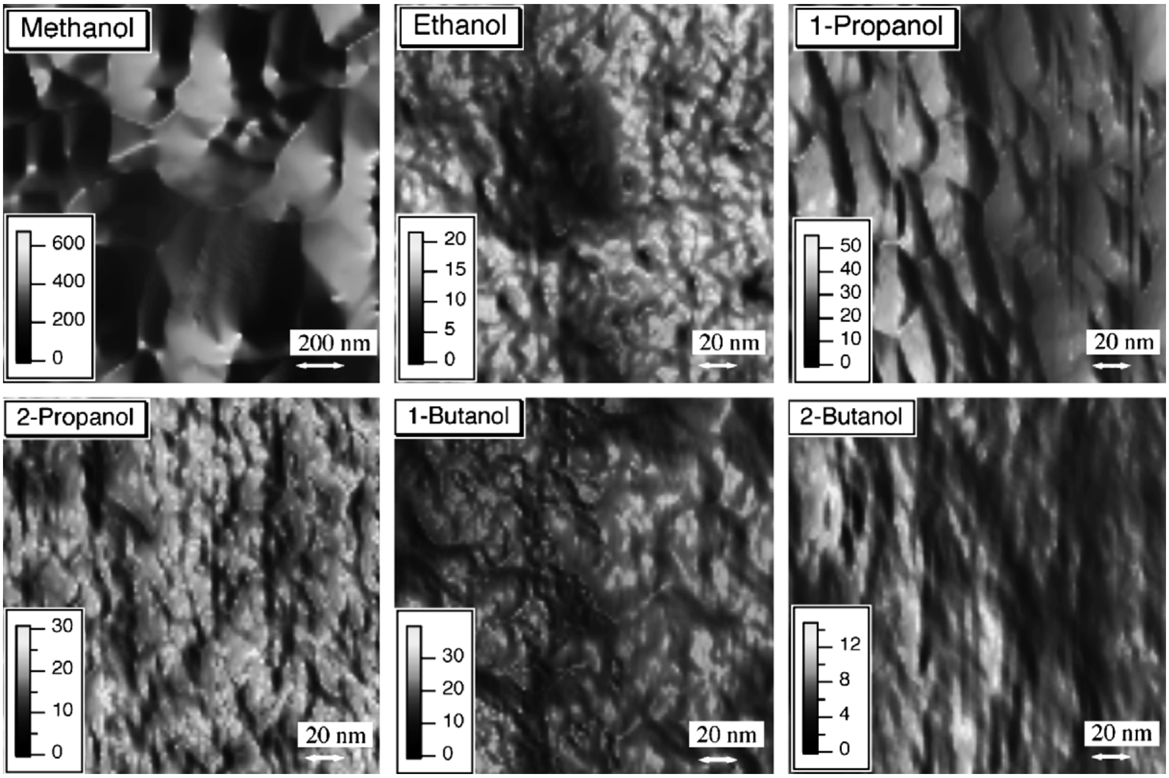

Fig. 4. AFM surface topographies for the TES-Oct/PWA membranes prepared under various types of alcohol.

2.2.4. *Conductivity measurement*

Proton conductivity measurements were performed on a Hioki 3532-80 impedance analyzer couple with two platinum electrodes placed in a thermostat chamber (Espec Co. Ltd., LHL-113) at 60 °C/95%RH. The conductivity was determined from Cole–Cole plot by an AC impedance method in the range 10 Hz–1 MHz. The measurements were iteratively carried out until the impedance reached the plateau value.

3. Results and discussion

Fig. 1 shows the proton conductivity, σ, for the TES-Oct/PWA membranes prepared under different kinds of alcohol. While the most of the data reached sufficient level applicable for proton conductive membranes, that are prepared in methanol resulted in $\sigma \sim 10^{-5}$ (S/cm), which was three decades lower than others. Methanol, which has been considered to be suitable to maximize the functionality of the PWA anion as a catalyst, is widely used as polar solvent for sol–gel synthesis. However, it may not be applicable for the present system consisting of an organically modified alkoxide with PWA because phase separation takes place before reaching the gel point. Such a phenomenon might occur due to the fact that one of the alkoxide group is replaced by an alkyl bridge, that leads to the formation of less condensed structure by rapid chain growth rather than hyper branching. In addition to such an inductive effect of the alkyl group [1], the fast evaporation of the solvent could lead to the phase instability upon increasing concentration. Note that if the hydrogen bond has an additional role to the reaction [11], e.g., prohibiting the reaction front of the silanol groups, the alkoxide may form further less branched structure by extending its chain ends. In any case, most of the PWA could leak during the structural formation if phase separation takes place before stabilizing the network structure.

In order to understand the variation of the proton conductivity for the hybrid membranes prepared under different kinds of solvents, the amount of PWA successfully incorporated in the membrane was investigated by titration. In general, the hydrated water in PWA depends on the temperature and the relative humidity. Their role is to compensate for the charge potential of the huge PWA anion [14]. Since the amount of base required to neutralize the strong acid was unknown, the known amount of PWA was titrated by using sodium hydroxide as shown in Fig. 2(a). Thus the amount of PWA successfully introduced into the membrane, W_{PWA}, was estimated from the amount of leaked PWA using a calibration curve. Fig. 2(b) shows W_{PWA}s obtained for different types of solvents. W_{PWA} increased in the order methanol < 1-butanol < 2-propanol < ethanol < 1-propanol < 2-butanol which was reminiscent of the proton conductivity as demonstrated in Fig. 1. While the conductivity was almost dependent on the amount of PWA, it is interesting to examine the network structure by SAXS, AFM and TGA to consider their effects on the proton conductivity.

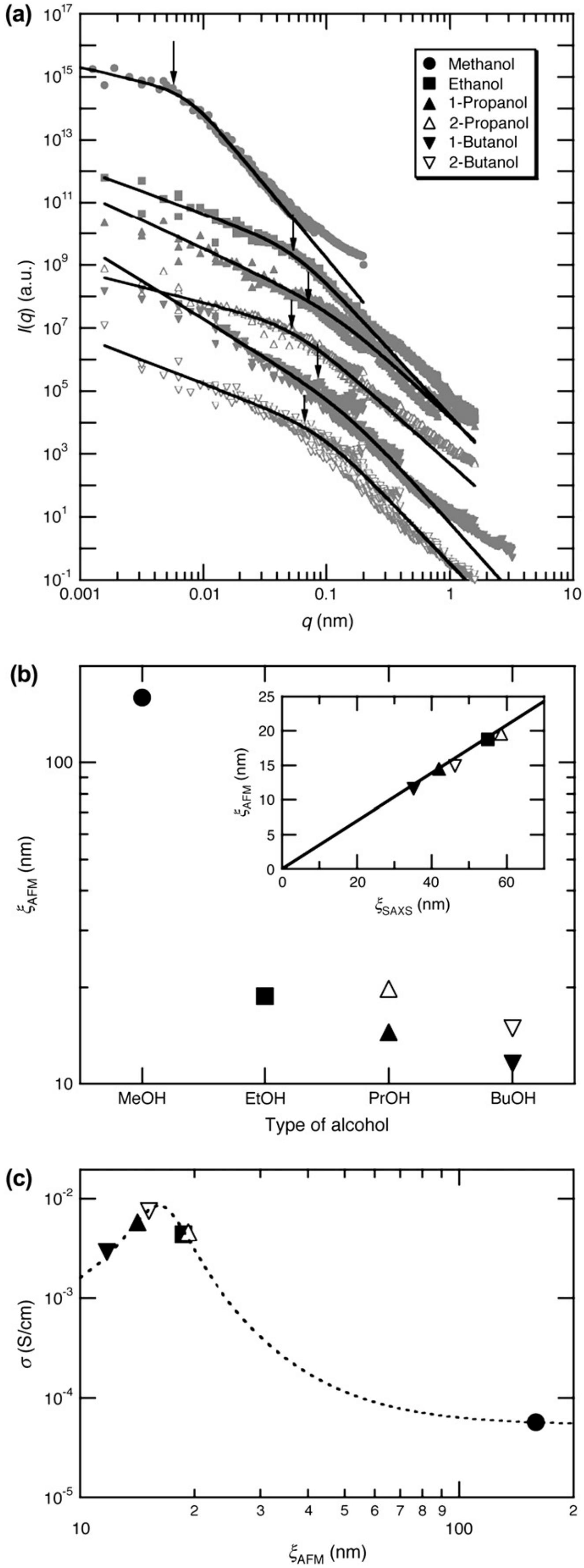

Fig. 5. (a) Power spectra obtained from the two-dimensional FFT of the AFM images for the TES-Oct/PWA membranes prepared under various types of alcohol. (b) ξ_{AFM} evaluated from the FFT analysis. The inset shows the linear relation between ξ_{AFM} and ξ_{SAXS}. (c) Plot of σ as a function of ξ_{AFM}.

Fig. 3(a) shows the SAXS profile for the TES-Oct/PWA membranes observed at room temperature, where $I(q)$ is the intensity observed at the magnitude of the wave vector q. The inset shows the result for the HCl-catalyzed membrane as a control. Since the scattering peak appeared in the absence of PWA, this peak can be attributed to the inter-domain (or inter-void) distance of the TES-Oct/PWA clusters rather than the aggregated structure of PWA itself although tungsten can be a good contrast agent due to the high electron density. A SAXS correlation length, ξ_{SAXS}, was estimated from the peak location, q_{max}, by the following equation:

$$\xi_{SAXS} = 2\pi/q_{max} \tag{1}$$

Fig. 3(b) shows ξ_{SAXS}s for different types of alcohol. Note that the TES-Oct/PWA membrane prepared in methanol is opaque, indicating a very strong light scattering. Therefore the scattering peak of the methanol membrane was not detectable in this experiment range of the wave vector. ξ_{SAXS} decreased with the number of carbons of alcohol as a general trend and those for isoform solvent exhibited the larger value.

In order to ensure that the SAXS analysis provided a valid correlation length, an alternative approach was taken. Fig. 4 shows the surface morphologies for the TES-Oct/PWA membranes observed by AFM. Except that the methanol membrane exhibits obviously large structure, it is quite difficult to envisage how the solvent affects the structure with quantitative understanding solely from the surface images. Thus, those images were further analyzed by an FFT analysis to evaluate a characteristic length below.

Fig. 5(a) shows the power spectra of the AFM images for the TES-Oct/PWA membranes prepared in different solvents obtained by radially averaging the two-dimensional FFT images with the different scanning sizes, where the solid lines indicate the fitting results with the following equation [7,15,16]:

$$I(q) = \frac{1}{k_0(q\xi_{AFM})^{2(1+2\alpha)} + k_1(q\xi_{AFM})^{\beta}} \tag{2}$$

where ξ_{AFM}, α and β are the characteristic length for AFM, the self-affine exponent and another exponent to represent the higher order structure. k_0 and k_1 are relative strength for each contribution. The arrows indicated the characteristic wave vector q corresponding to the reciprocal of ξ_{AFM}. Fig. 5(b) shows ξ_{AFM} for different types of alcohol, where the inset shows the relation between two correlation functions obtained by SAXS and AFM. Since ξ_{AFM} is proportional to ξ_{SAXS}, this result suggests that the structural information is successfully extracted to discuss the effect of solvent upon microscopic structure for a series of the TES-Oct/PWA membranes. It is noted that ξ_{AFM} for methanol solvent is analyzable, suggesting AFM can be a complementary tool of SAXS for quantitative structure analysis. While the structural parameters were successfully evaluated from SAXS and AFM, those data exhibited a rather monotonic dependence. Fig. 5(c) shows the correlation between the proton conductivity and microstructure. The proton conductivity, σ, increased with ξ_{AFM} for the smaller domain structure ($\xi_{\mathrm{AFM}} < 15$ nm), followed by a decrease in σ as the domain size became larger. The figure indicates that the better proton conduction requires a well-developed domain structure, which can be induced by incorporation of the larger amount of PWA as we reported earlier [7]. However, further increase in ξ_{AFM} led significant reduction of σ. This is probably due to a coarse network structure attributed to the unstable structural formation. Thus further structural investigation is required to elucidate how the solvents affect the functionality and internal structure of the materials.

Besides SAXS and AFM indicated the characteristic size of the microscopic structure, TGA measurements may provide us useful insight into the average degree of cross-linking or the microscopic structure inside the domains. As reported earlier [7], the weight loss from the TES-Oct/PWA membranes, which are directly related to the rigidity or branching degree of the network structure, can be attributed to the disintegration of the organic bridge. The analysis was applied to the series of TES-Oct/PWA membranes prepared under different alcohols. Fig. 6(a) shows the weight derivative with respect to the temperature for a series of the TES-Oct/PWA membranes. The characteristic temperature increased in the order methanol < 1-butanol < 2-butanol < 1-propanol<ethanol < 2-propanol. Although the characteristic temperature for TGA decreased with the number of carbon atoms of alcohol the methanol system exhibited exceptionally low value compared with any other samples. When the sol–gel reaction was carried out in the presence of methanol as a solvent, the resultant membrane was opaque, suggesting that the network was in the phase separated and loosely cross-linked states. The reactor batch became opaque from the beginning of the reaction when the gelling test was performed by using the test tube inversion method. Thus, the fast evaporation of solvent is not the main reason for this result. It is well known, that sol–gel reaction is accelerated when one of the four alkoxide groups is replaced by alkyl group as the so-called induction effect [1]. If the chain extension proceeds preferentially compared with the branching (cross-linking) reaction, the system becomes unstable with respect to the concentration fluctuations, where the cross-linking has an important role in stabilizing the concentration fluctuations. Therefore, the TES-Oct/PWA membrane prepared by methanol may form coarse and low cross-linking domains as indicated, respectively, by the results obtained by AFM and TGA. In this case, it is reasonable to consider that most of the PWA could leak out from the membrane during the course of sample preparation. From the

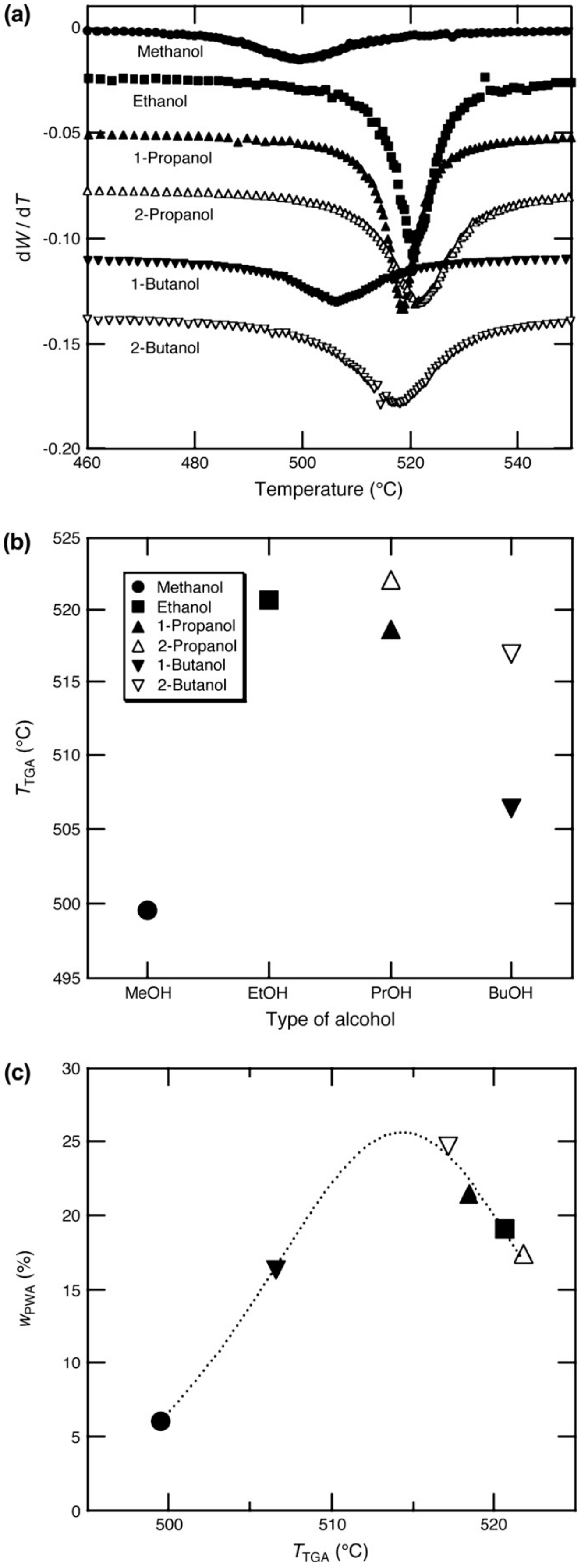

Fig. 6. (a) Weight derivative with respect to the temperature in different solvents. (b) T_{TGA} for various types of solvent. (c) Plot of W_{PWA} as a function of T_{TGA}.

TGA experiments, it was found that there is an optimal condition for the amount of PWA in the membranes. In this study, it was found that 2-butanol is the best solvent to prepare the proton conductive membrane consisting of the organic–inorganic components. The high viscosity or the boiling temperature of the solvent would be necessary to produce a well-developed domain containing a sufficient amount of PWA without macroscopic segregation.

4. Conclusions

Methanol is a commonly used solvent to prepare membranes via the sol–gel synthesis of tetraalkoxide. Since the cyclization or intra-domain cross-linking dominates the reaction rate of the alkoxide, it could be one of the best solvents to maximize the performance of acid or base catalyst in the sol–gel processing. However, in the case of sol–gel derived organic–inorganic hybrids, because of the presence of the organic bridge, the TES-Oct/PWA membrane in the presence of methanol resulted in highly phase separated state, leading to serious leaking of the proton conductor, PWA. The incorporated amount of PWA seemed to have an optimum value with respect to the TGA characteristic temperature. This suggests that the cross-linking degree or the structure should be moderate, i.e., not too loose nor too tight to produce the better proton conductive membrane via the sol–gel reaction. SAXS and AFM can provide structural insight whereas the titration technique gives the concentration of PWA in the membrane. Therefore, all the techniques are required to understand the functionality of the membrane. An AFM accompanied by Fourier analysis can be a powerful tool to quantitatively evaluate the microscopic structure complementary to the scattering techniques.

Acknowledgments

This work is supported by Grant-in-Aid, no. 16750189 from the Ministry of Education, Science, Sports, Culture, and Technology.

References

[1] Brinker CJ, Scherer GW. Sol–gel science. London: Academic Press; 1990.

[2] Stober W, Fink A, Bohn E. J Colloid Interface Sci 1968;26:62–9.

[3] Sanchez J, McCormick AV. J Non-Cryst Solids 1994;167:289.

[4] Loy DA, Carpenter JP, Alam TM, Shaltout R, Dorhout PK, Greaves J, et al. J Am Chem Soc 1999;121(23):5413.

[5] Loy DA, Carpenter JP, Myers SA, Assink RA, Small JH, Greaves J, et al. J Am Chem Soc 1996;118:8501.

[6] Shea KJ, Loy DA. Chem Mater 2001;13:3306.

[7] Nakanishi T, Norisuye T, Sato H, Takemori T, Tran-Cong-Miyata Q, Nomura S, et al. Macromolecules 2007;40:4165–72.

[8] Aoki Y, Norisuye T, Tran-Cong-Miyata Q, Nomura S, Sugimoto T. Macromolecules 2003;36(26):9935–42.

[9] Takata Y, Norisuye T, Hirayama S, Takemori T, Tran-Cong-Miyata Q, Nomura S. Macromolecules 2007;40:3773–8.

[10] Norisuye T, Inoue M, Shibayama M, Tamaki R, Chujo Y. Macromolecules 2000;33:500.

[11] Sadasivan S, Dubey AK, Li Y, Rasmussen DH. J Sol-Gel Sci Technol 1998;12:5–14.

[12] Bernards TNM, van Bommel MJ, Boonstra AH. J Non-Cryst Solids 1991;134:1–13.

[13] Weissberger A. Organic solvents: physical properties and methods of purification. In: Techniques of chemistry, vol. 2. New York: Wiley-Interscience; 1986.

[14] Moffat JB. Metal-oxygen clusters: the surface and catalytic properties of heteropoly oxometalates. New York: Kluwer Academic/Plenum Publishers; 2001.

[15] Yang H-N, Wang G-C. J Appl Phys 1993;74(1):101–6.

[16] Zad AI, Kavei G, Tbar MRR, Allaei SMV. J Phys Condens Matter 2003;15:1889.